

Supplementary material

A Healing Promotion Wound Dressing with Tailor-made Antibacterial Potency employing piezocatalytic processes in multi-functional nanocomposites

Yi Zhang^a, Qi An^{a,}, Shuting Zhang^a, Zequn Ma^{a,d}, Xiantong Hu^{b,c}, Mengchun Feng^{b,c}, Yihe Zhang^a, Yantao Zhao^{b,c,*}*

^a Beijing Key Laboratory of Materials Utilization of Nonmetallic Minerals and Solid Wastes, National Laboratory of Mineral Materials, School of Materials Science and Technology, China University of Geosciences, Beijing, 100083, China.

^b Senior Department of Orthopedics, the Fourth Medical Center of PLA General Hospital, Beijing 100048, China

^c Beijing Engineering Research Center of Orthopedics Implants, Beijing 100048, China

^d Institute of Materials Science and Devices, Suzhou University of Science and Technology, Suzhou, 215000, PR China

E-mails: an@cugb.edu.cn; userzyt@qq.com

Section S1. Experimental section.

Section S2. The β -phase fractions calculated of the samples.

Section S3. Figures and tables.

Section S1. Experimental section.

Materials: Poly(vinylidene fluoride-co-hexafluoropropylene) (PVDF–HFP) (density 1.78 g cm⁻³, 5–20% molar of hexafluoropropene) and CNT were purchased from Sigma–Aldrich. PPy was purchased from Aladdin. CB, N,N-dimethyl formamide (DMF, P99.5%) and all other reagents were obtained from Sinopharm Chemical Reagent Beijing Co., Ltd (Beijing, China). The reagents were all analytical grade and used without further purification. For cell culture, the L929 cells were obtained from the Chinese Academy of Medical Sciences. Fetal bovine serum (FBS) was purchased from Sangon Biotech Co. (Shanghai). Calcium⁺ and magnesium-free phosphate buffered saline (PBS), trypsin and dulbecco's modified eagle medium (DMEM) were obtained from Thermo Fisher Scientific Inc. (USA). Paraformaldehyde and dimethyl sulfoxide (DMSO) were obtained from Beijing Chemical Plant (Beijing, China).

Preparation of the smooth piezoelectric CF: PVDF-HFP (1 g) particles were dissolved in 4 mL DMF, then stirred at 80°C for 30 min to obtain a PVDF-HFP solution. A certain amount of CB was added to the PVDF-HFP solution to obtain a mixture with the specific amount of CB fractions. The dispersion homogenized under ultrasonication and kept for 2 h at 80 °C with stirring. Finally, mixture was casted into a film and kept in an oven at 80 °C for 3 h to evaporate the solvent. The composite film with high piezoelectric performance (high fraction of β-phase) was thus obtained.

Preparation of the porous piezoelectric CF: The porous CF was prepared using a phase-inversion process. PVDF-HFP (1 g) particles were dissolved in 4 mL DMF, then stirred at 80°C for 30 min to obtain a PVDF-HFP solution. A certain amount of CB was added to the PVDF-HFP solution to obtain a mixture with the specific amount of CB fractions. The transparent solution was casted onto a glass substrate and immersed into a water bath to undergo phase inversion. The PVDF-HFP film was peeled off from the glass substrate and washed several times with deionized water.

The adsorption and release of molecules: Aqueous solutions of 1 mg·mL⁻¹ of the molecules

riboflavin, LA, and Dex were prepared as the feeding solutions. The PPy/CNT@CF were immersed into the feeding solutions for 24 h to reach equilibrium absorption. All the multilayers were rinsed briefly in deionized water to remove superficially absorbed molecules after the loading step. Then films were immersed in a phosphate buffer solution (PBS) to release the loaded molecules. During the release processes, piezoelectricity was generated by pressing the multilayers based on the piezoelectric film. The absorbances of the release solution were monitored at specific time by taking 3 mL solution out for the measurement and the solutions were returned after measurement.

In vitro ROS detection: The amounts of $O_2^{\cdot-}$, $\cdot OH$ and H_2O_2 generated under the irradiation of ultrasonic were determined by nitroblue tetrazolium (NBT) transformation, terephthalic acid photoluminescence (TA-PL) and iodide method, respectively. The ultrasonic irradiation derived from an ultrasonic cleaner (KQ-300DE, 240 W). NBT can react with $O_2^{\cdot-}$ and displaying a maximum absorbance at 259 nm, thus can be used to ascertain the generated amount of $O_2^{\cdot-}$ over catalysts by recording the reduction of NBT on an UV-5500PC spectrophotometer. Terephthalic acid (TA) is a well probe molecule for detecting $\cdot OH$ radicals due to their reaction production has a specific fluorescence emission maximum at wavelength of 425 nm. The amount of $\cdot OH$ radicals can be determined by measuring the fluorescence intensity at 425 nm with the excitation wavelength of 315 nm on a fluorescence spectrophotometer (F97XP, China). The $O_2^{\cdot-}$ and $\cdot OH$ quantification experiments are performed as follows: the samples (1 cm \times 3 cm) were dispersed into 100 mL of NBT (0.025 mM) or TA (0.5 mM) solution in a 250 mL quartz beaker. The temperature of this system was kept at 25 °C by frequent water inflow and outflow operation. At every 30 min ultrasonic, about 4 mL of the solution was taken and was analyzed on an UV-5500PC spectrophotometer or a fluorescence spectrophotometer (F97XP, China).

In vitro H_2O_2 ROS detection: A chromogenic reaction was conducted to detect the yield of H_2O_2 using TMB as a chromogenic agent. In detail, the samples were added into pure water or ethanol

solution for ultrasonic irradiation in an ultrasonic cleaner (KQ5200DE, 160 W). Every hour, 500 μ L of the ultrasonicated solution was mixed with 100 μ L of a 10 mg/mL TMB solution in dimethylsulfoxide and 1.8 mL of acetic acid/sodium acetate buffer (pH 3.6), and then 20 μ L of a 100 μ g/mL horseradish peroxidase solution was added. After 30 min, the yield of H_2O_2 was determined by measuring the absorbance at 652 nm on an UV-vis spectrophotometer.

Cell adhesion assay: L929 cells were cultured in high glucose DMEM supplemented with 10% FBS and antibiotic- antimycotic solution containing 100 U mL^{-1} penicillin and 100 U mL^{-1} streptomycin sulfate. The culture conditions were a humidified atmosphere of 5% CO_2 and 95% air at 37°C. A piece of the piezoelectric-LbL film (1 cm*1 cm) was placed in a cavity of a 24-well plate and adding 1 ml cell suspension after (the density is $1*10^5$). The piezoelectric group is vibrated by the beauty device for 1 h. Prior to seeding cells, the samples were sterilized under Co 60 (γ) laser for 30 min. After incubation for 24 h, cells were stained with the LIVE/DEAD Viability/Cytotoxicity Kit for 10 min and washed with PBS for three times to remove free dyes to observe the number and morphology of the cells. The cells attached to the sample and the well plate were observed.

Cytotoxicity Study: For the cytotoxicity of samples, L929 cells were seeded in a 48-well tissue culture polystyrene plate (TCPS) at a density of 10000 cells per well for 24 hours. After that, sample's extracts were added into the DMEM. The L929 and samples were further incubated at 37°C for 3 days. To determine the cytotoxicity of samples, 100 μ L of CCK-8 (final dilution: 1:10), which can react with dehydrogenase in mitochondria to form a water-soluble formazan, was added onto the medium to evaluate the viability. Afterwards, 100 μ L of the supernatant was transferred into a 96-well plate to measure the absorbance at 490 nm.

In vivo antibacterial and wound repair: Balb/c mice (male, 6 weeks, ~20 g body weight) were obtained from Fourth Medical Center of the General Hospital of CPLA. Firstly, the mice were anesthetized by intraperitoneal injection of 0.3% pentobarbital sodium with a dose of 45 mg kg^{-1} body weight. Then, the dorsal hair of mice was shaved and a rounded full-thickness skin

wound ($d = 8$ mm) was created. After, the wounds were infected with $20 \mu\text{L}$ (10^7 CFU mL^{-1}) *S. aureus* for 1 day (denoted as day 0). The wound infection was confirmed by the routine swab culture and spread plate method. Finally, the successfully infected mice were randomly divided into two groups, control group, and PPy/CNT@CF group. For the PPy/CNT@CF group, the samples were covered on the wound and the massager shakes for ten minutes. The wound sizes of the animals were recorded. At the termination of the experiments, the animals were sacrificed. The skin tissues of the wound regions were retrieved.

For histological analysis, the dermal tissues surrounding the original wounds were retrieved, fixed with 10% formalin, embedded in paraffin, sectioned to obtain $8 \mu\text{m}$ pathological slides, and used for hematoxylin and eosin (H&E) staining, Masson's trichrome staining, CD31 immunohistochemistry staining. The images were analyzed and calculated by Image J.

Mouse wound model without bacterial infection was built following the same procedure as described above without bacterial infection.

Characterization: Atomic force microscopy (AFM) was obtained by scanning probe microscope. Scanning electron microscopy (SEM) measurements were carried out on a JSM-IT300 instrument. The piezoelectric response of the synthesized samples was characterized by an AFM (SPA-300HV) equipped with a ferroelectric test system. β -phase analysis of the polymeric film and the attenuated total reflection fourier transform infrared spectrum (ATR-FTIR) were conducted by the Bruker Tensor FTIR. Molecular releases and assemble process on quartz sheets were monitored using a UV-visible spectrum which obtained from a Hitachi U-3900H spectrophotometer. The output voltage and electrical current signals were recorded by a Keithley 2400 sourcemeter. Cell morphologies were observed using a Zeiss Leica inverted epifluorescence/reflectance laser scanning confocal microscopy. Electrochemical experiments were conducted in a three-electrode setup using 0.1 M PBS as the supporting electrolyte. The working electrodes were the multilayers assembled on the ITO-glass substrate, the reference electrode and the counter electrode were a silver chloride electrode and a Pt wire respectively.

Electron paramagnetic resonance (EPR) measurements were carried out using a Bruker E500 EPR spectrometer (Billerica, MA) at an ambient temperature.

Section S2. The β -phase fractions calculated of the samples.

The β -phase fractions of the samples were calculated by the portion of the vibrational bands of the α and β phases in FTIR according to equation S1.

$$F(\beta) = \frac{X(\beta)}{X(\alpha) + X(\beta)} = \frac{A_\beta}{1.26A_\alpha + A_\beta} \quad (\text{S1})$$

Where X_α and X_β were the α and β phases' crystalline mass fractions, and A_α and A_β were their absorption at 764 and 840 cm^{-1} . The 1.26 factor accounts for the ratio in absorption coefficients at 764 and 840 cm^{-1} .

Section S3. Figures and tables.

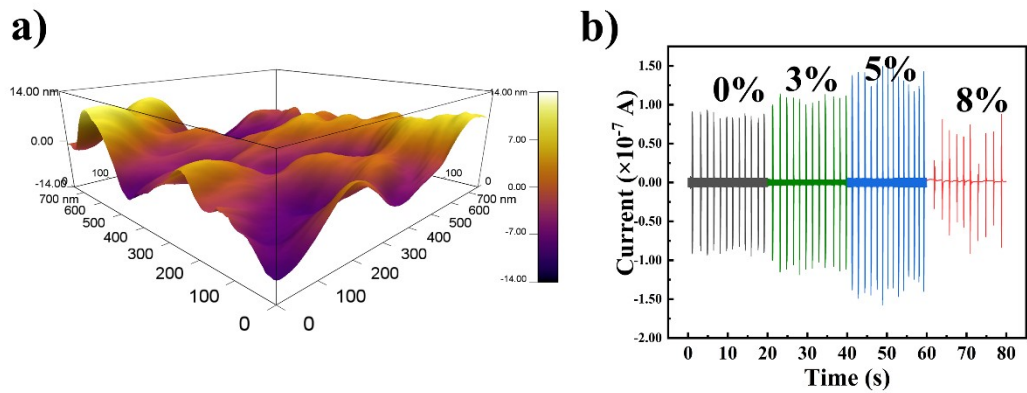


Figure S1. a) Morphological image of the self-powered CB/PVDF-HFP substrate. b) The short-circuit current under finger-pressing.

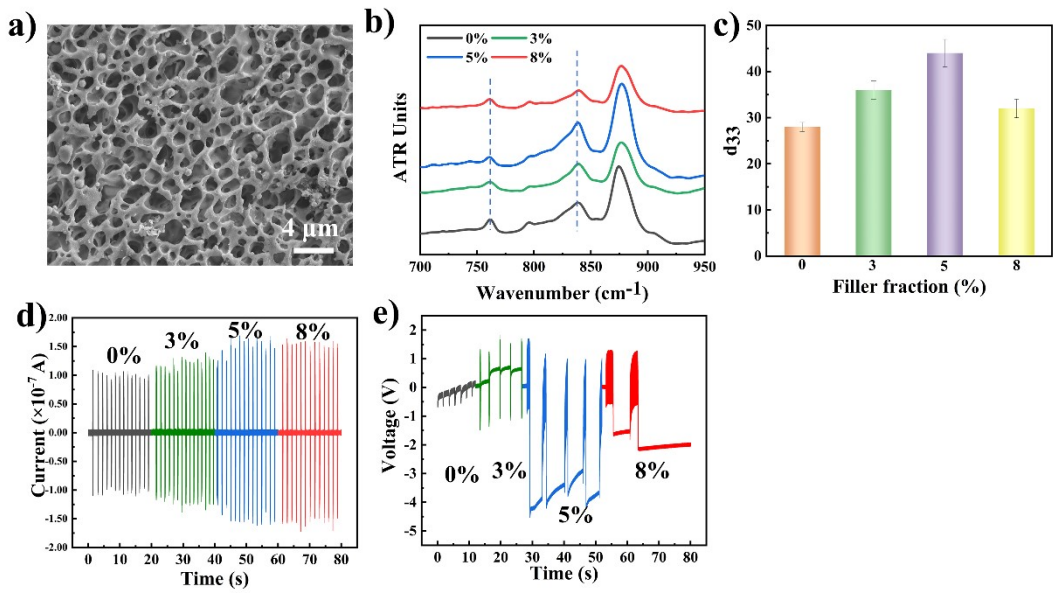


Figure S2. Characterization of the self-powered porous CB/PVDF-HFP. a) SEM image, b) FTIR spectra, c) d_{33} , d) short-circuit current under finger-pressing and e) open circuit voltages under finger-pressing of different filler-fraction PENGs.

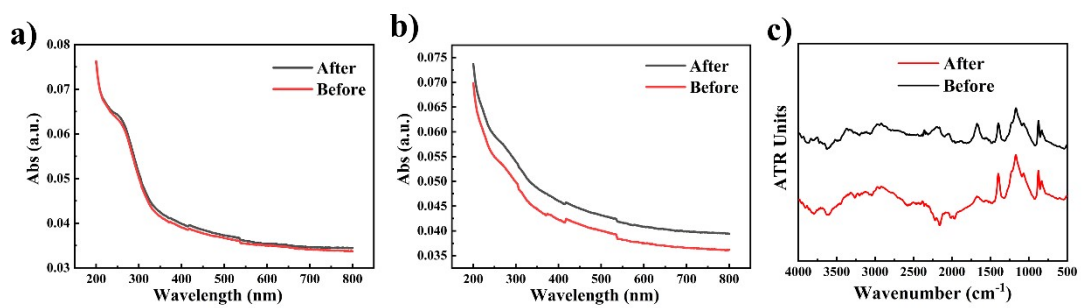


Figure S3. Stability of the multilayers. The UV-vis spectrum of the PPy/CNT multilayers a) immersed in the NaOH solution (pH 12) for 30 min and b) put into the aqueous solution for sonicating 5 min. c) ATR-IR spectra of PPy/CNT@CF before and after put into the aqueous solution for sonicating 5 min.

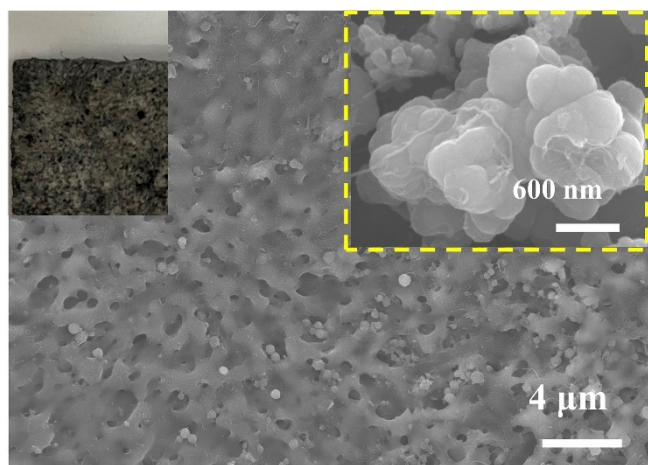


Figure S4. The SEM image of the multilayer film based on porous PENG.

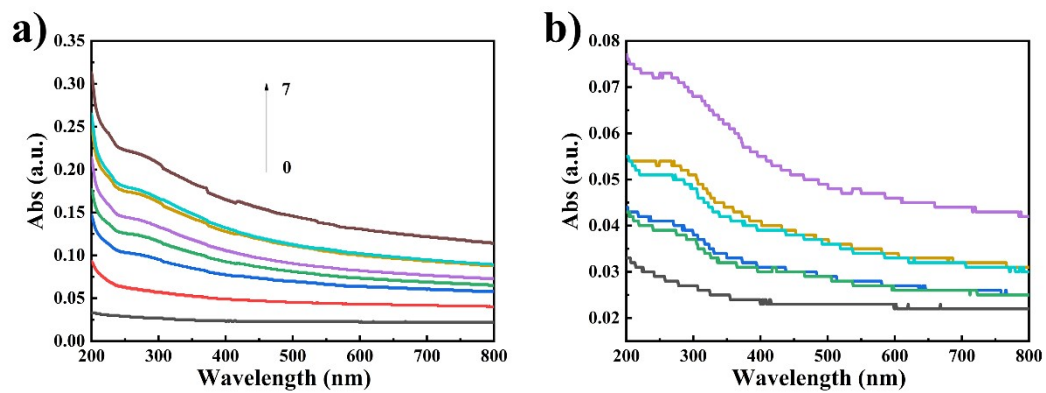


Figure S5. The UV-vis of the a) PAH/CNT and b) PANi/CNT multilayers along with the increase of bilayers.

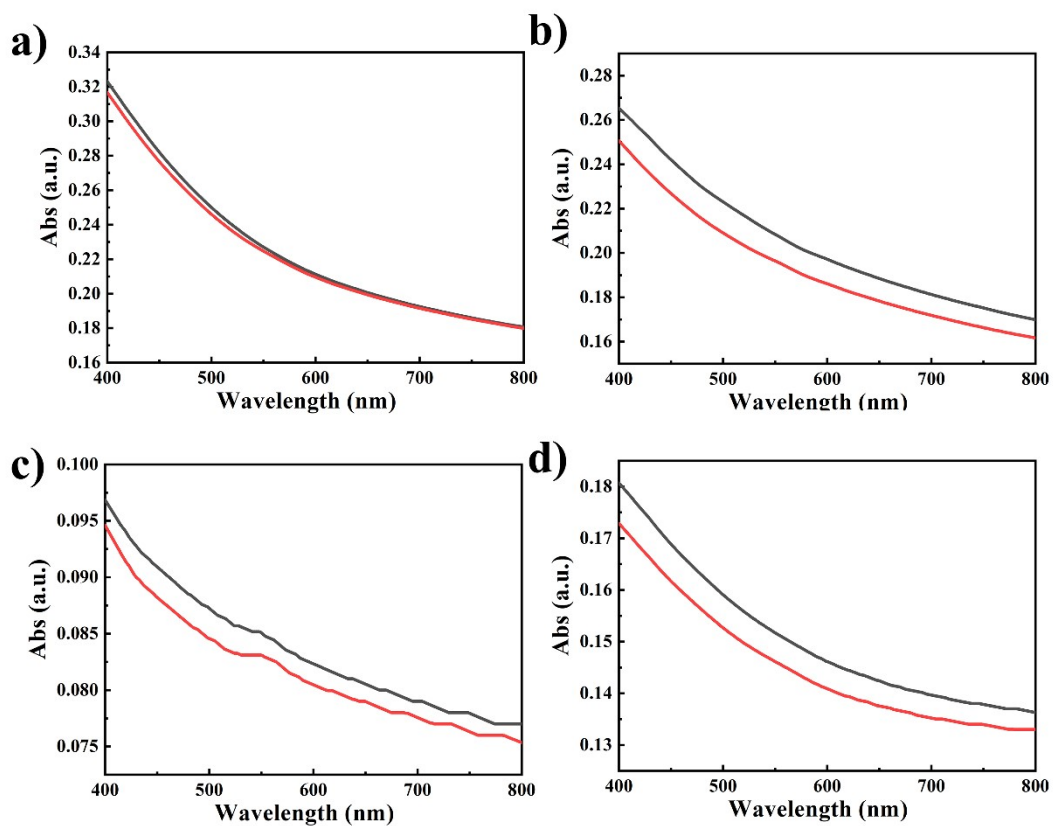


Figure S6. The UV-vis spectrum of the PAH/CNT and PANi/CNT multilayers before and after a-b) immersed in the NaOH solution (pH 12) for 30 min and c-d) put into the aqueous solution for sonicating 5 min.

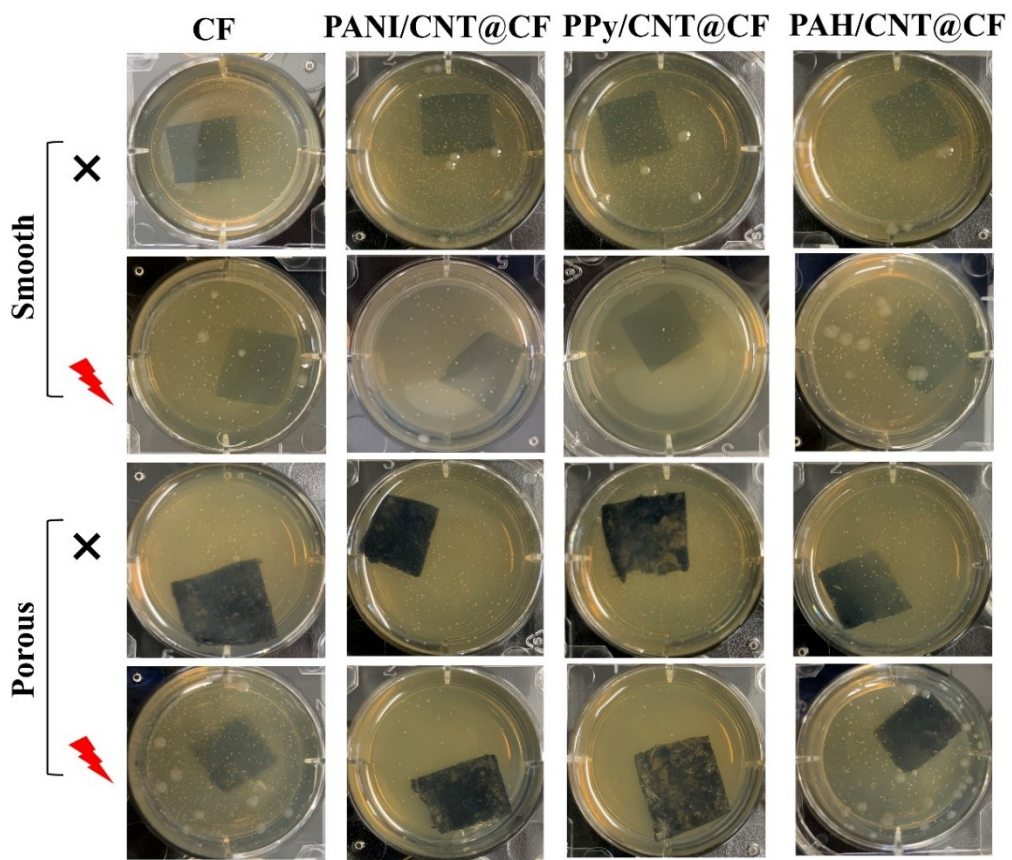


Figure S7. CFU comparison of different smooth and porous films against *S. aureus*.

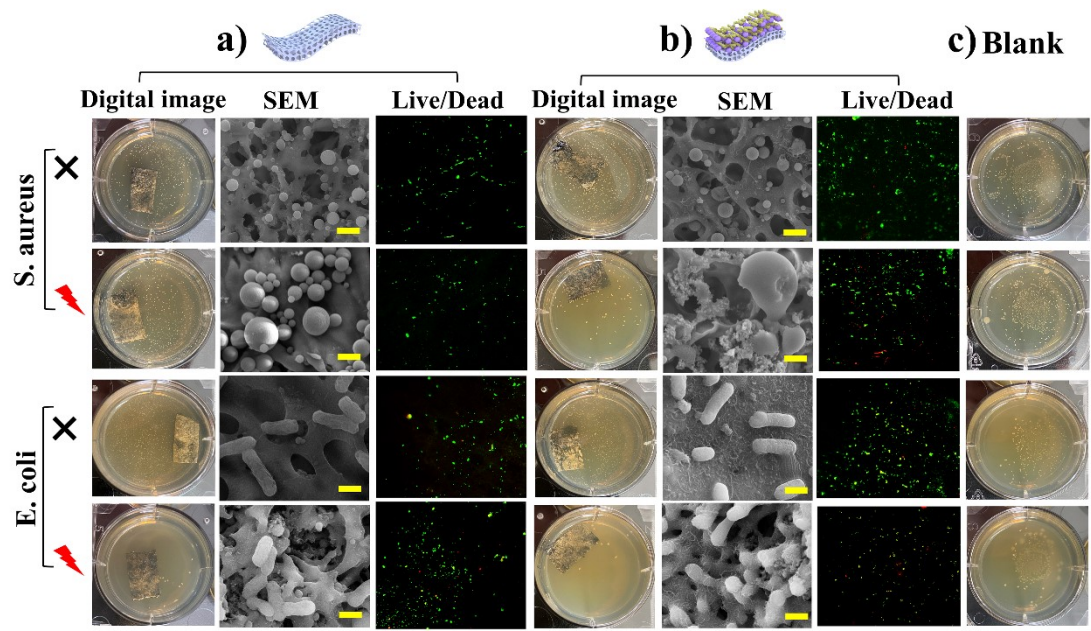


Figure S8. *In vitro* antibacterial effect of porous a) CF, b) PPy/CNT@CF and c) blank groups against *E. coli* and *S. aureus*.

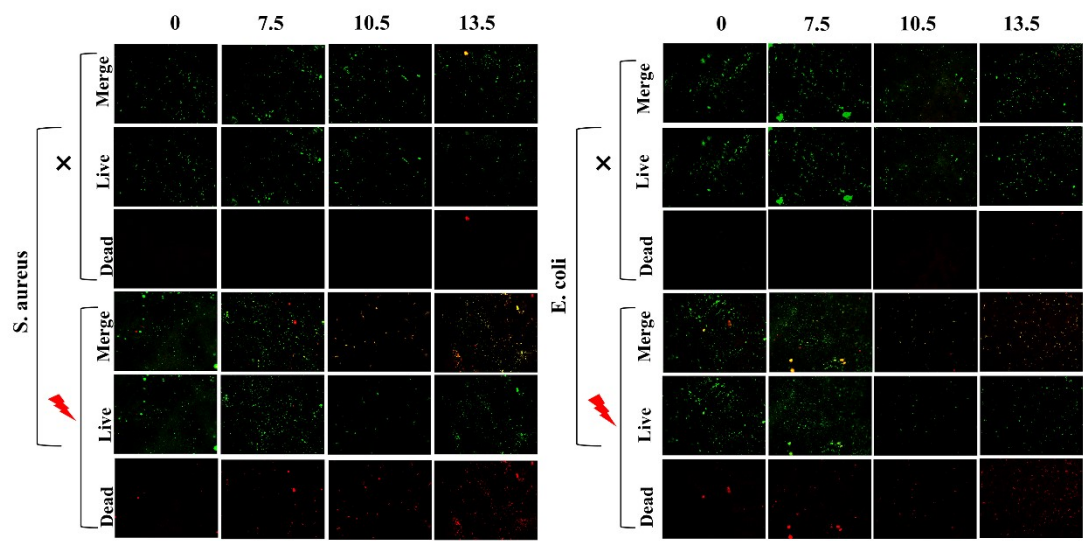


Figure S9. Live/dead staining images of different assemble-layer-number smooth films.

Table S1. The conductivities of different assemble-layer-number smooth films.

组装层数	0	7.5	10.5	13.5
电导率 (S/m)	4.27×10^{-5}	1.458×10^{-4}	3.18×10^{-4}	3.829×10^{-4}

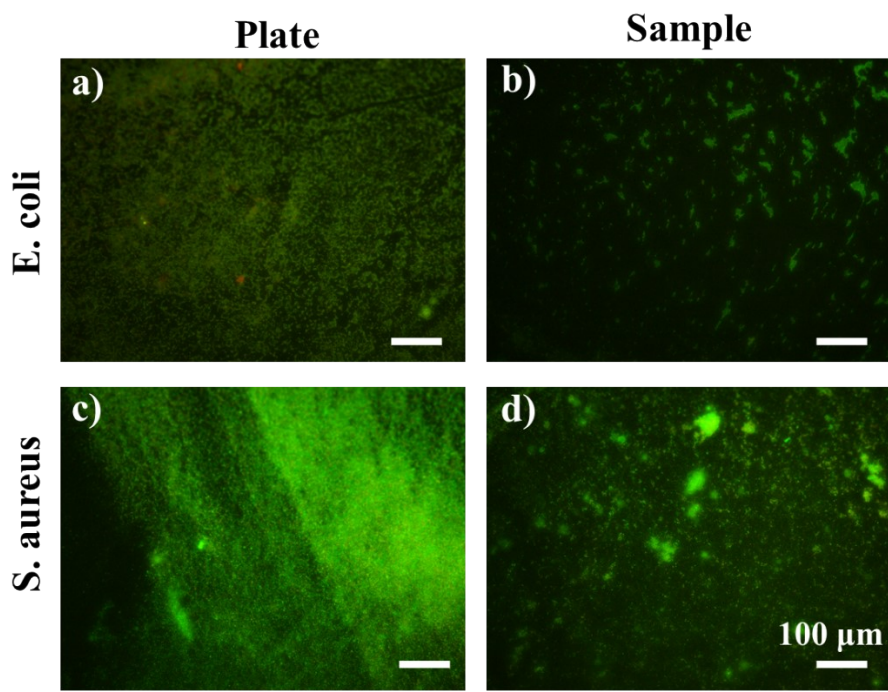


Figure S10. The antibiofilm performance of PPy/CNT@CF. Live/dead staining of a-b) E. coli and c-d) S. aureus on cell plate and samples after cultured 5 days.

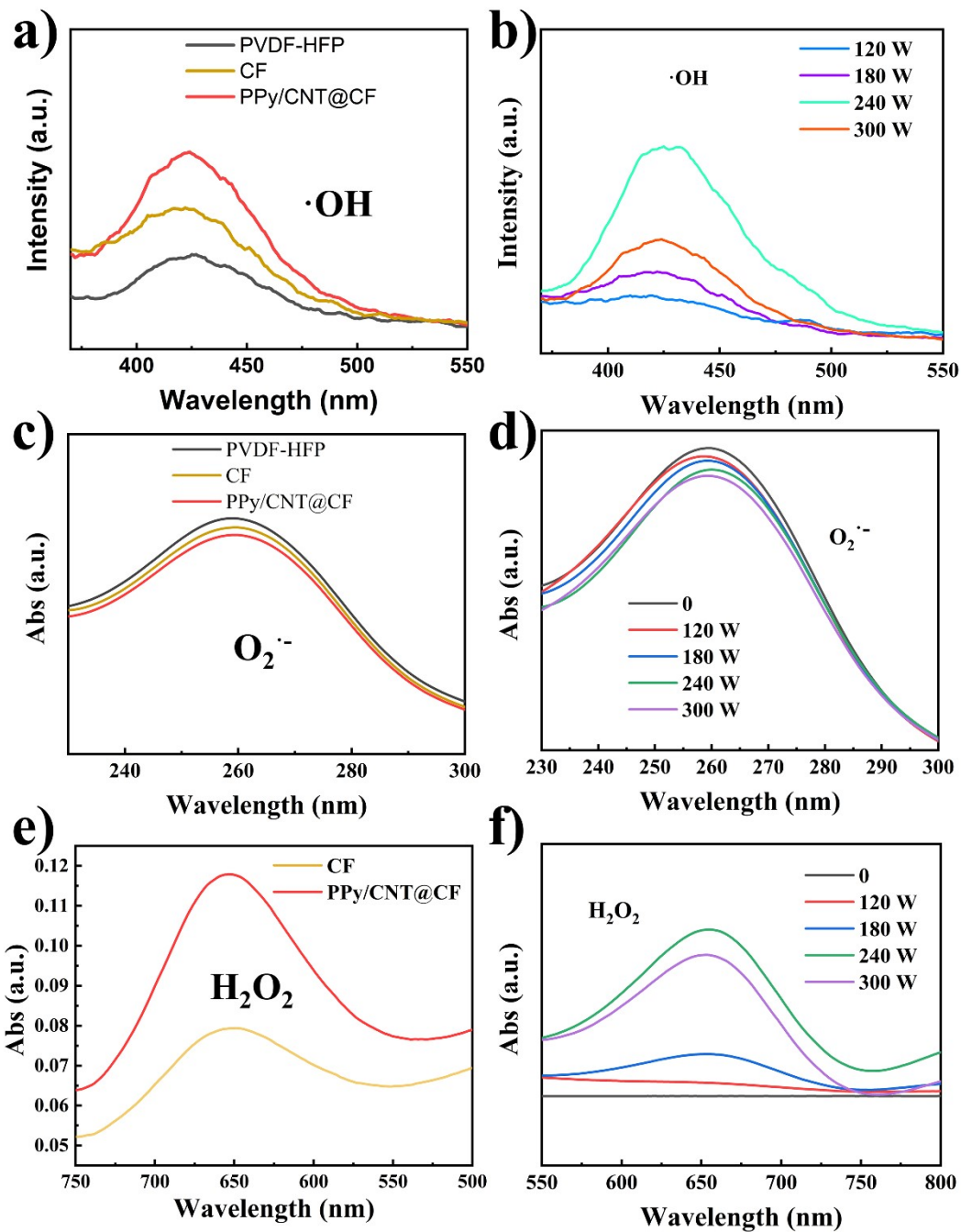


Figure S11. ROS generation for different films and the power dependence for ROS.

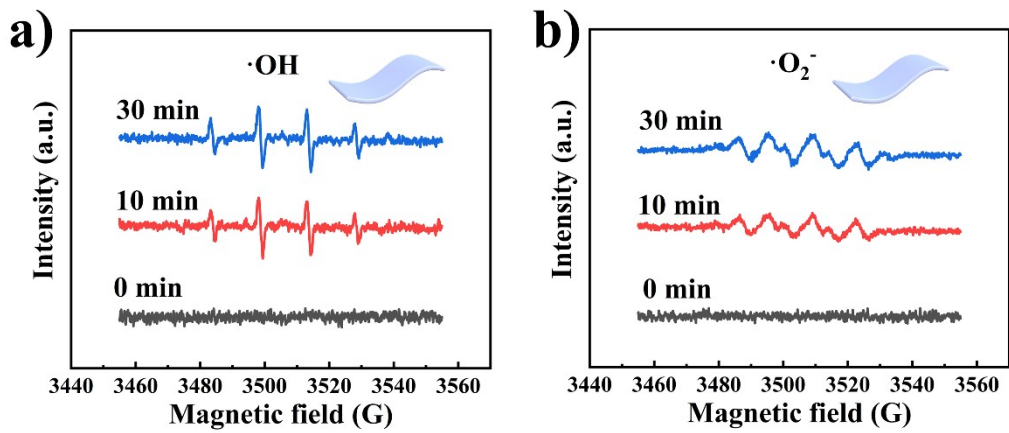


Figure S12. EPR measurements for a) •OH and b) O₂⁻ signal after different treatments of CF.

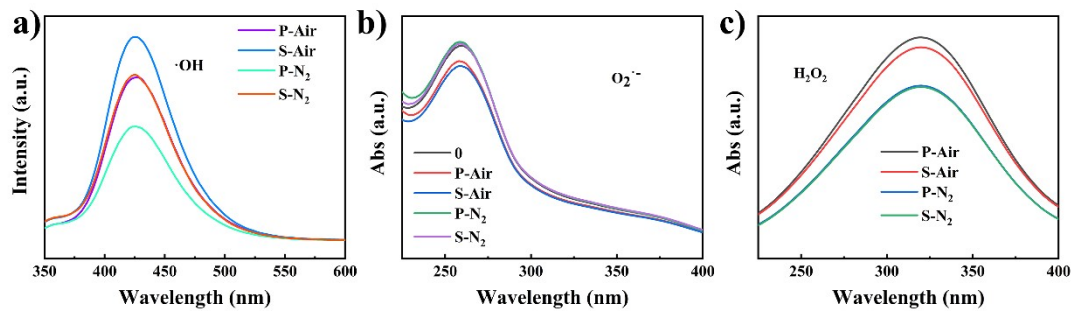


Figure S13. ROS generation with and without nitrogen.

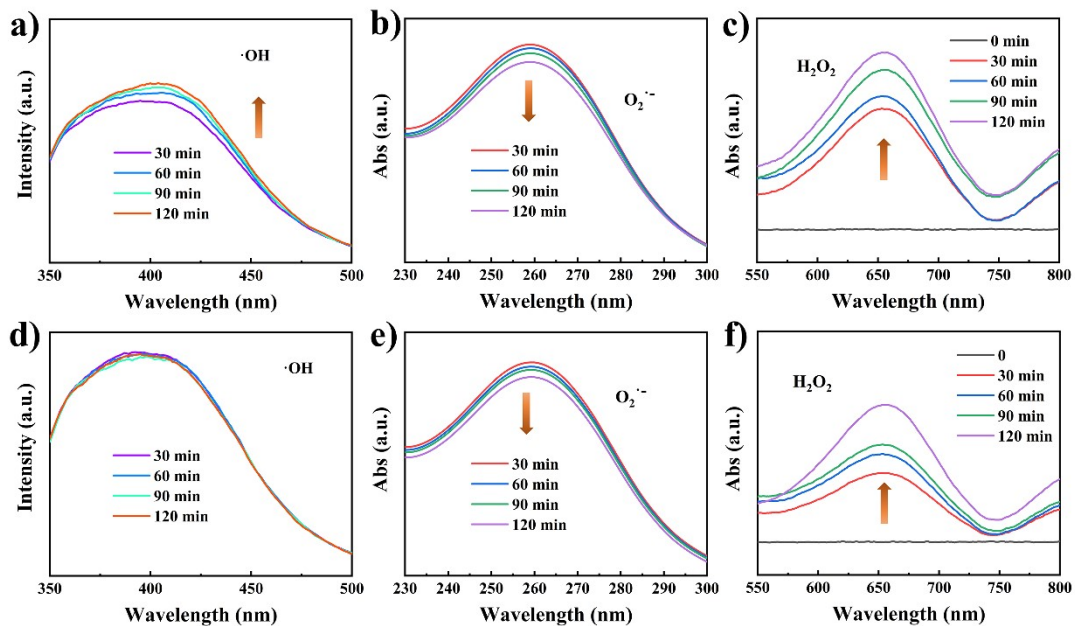


Figure S14. Time dependence for yield of ROS induced by a-c) electrochemical workstation and d-f) face-massage device.

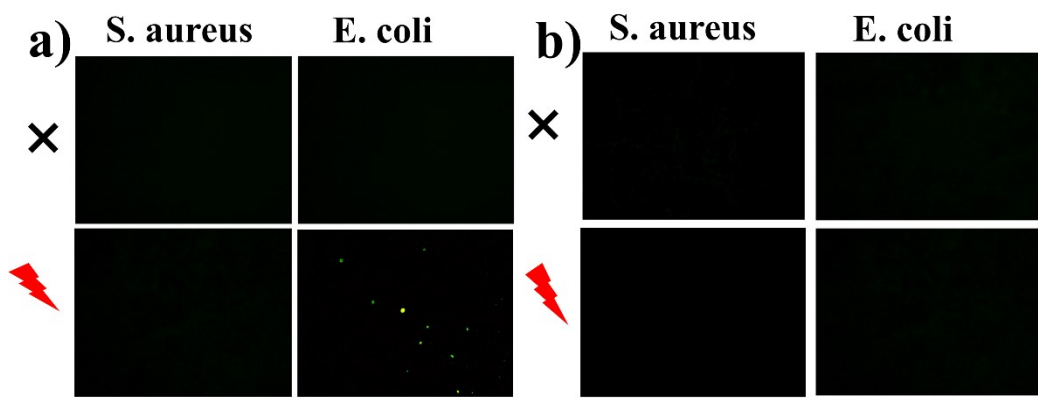


Figure S15. Detection of ROS production in bacteria of c) CF and d) pure PVDF-HFP.

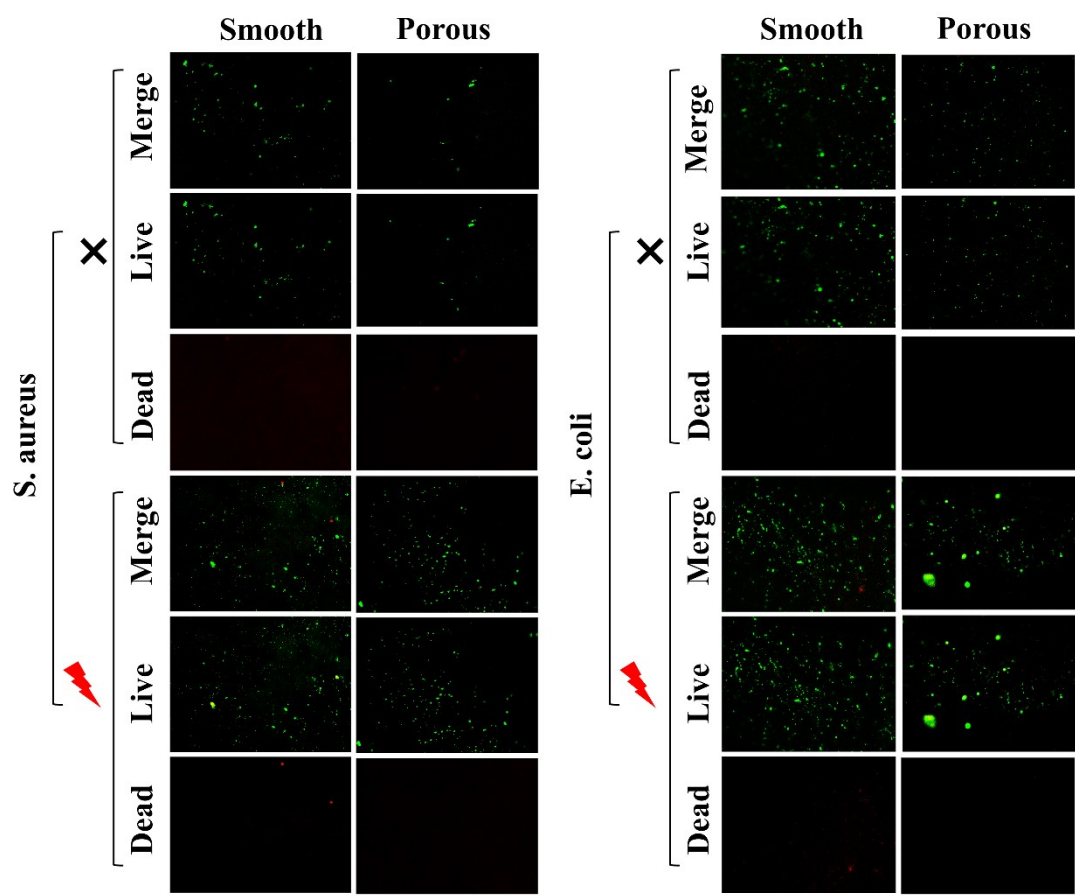


Figure S16. Live/dead staining images of pure PVDF-HFP films.

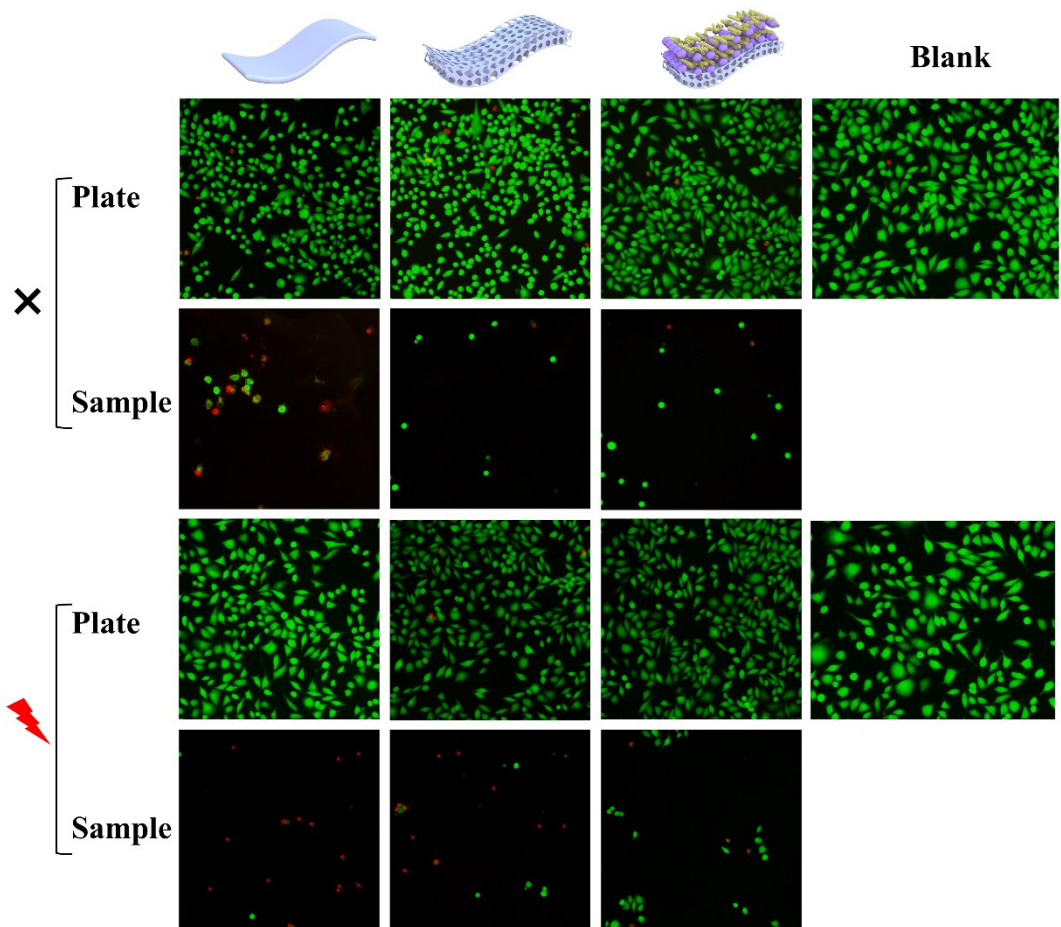


Figure S17. Live/dead cell staining of L929 cells of different samples.

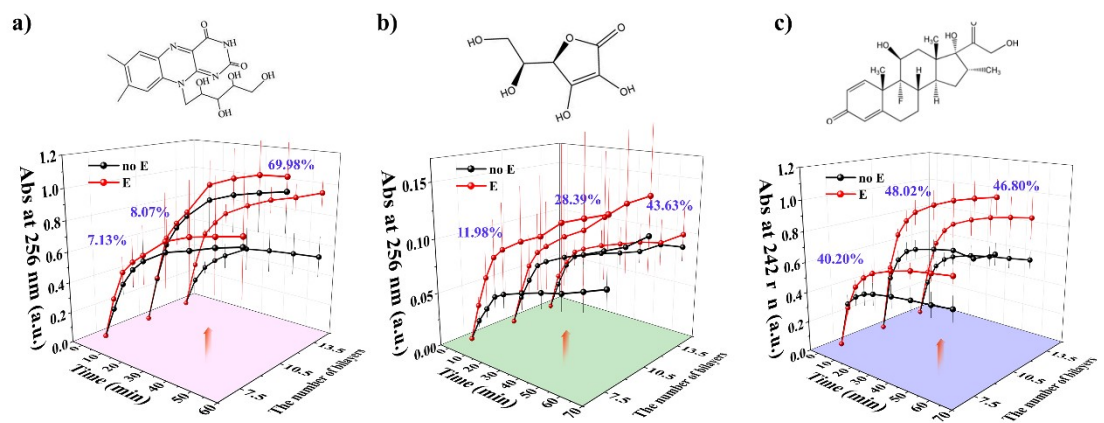


Figure S18. The releases of a) Riboflavin, b) LA, c) Dex with different bilayers.

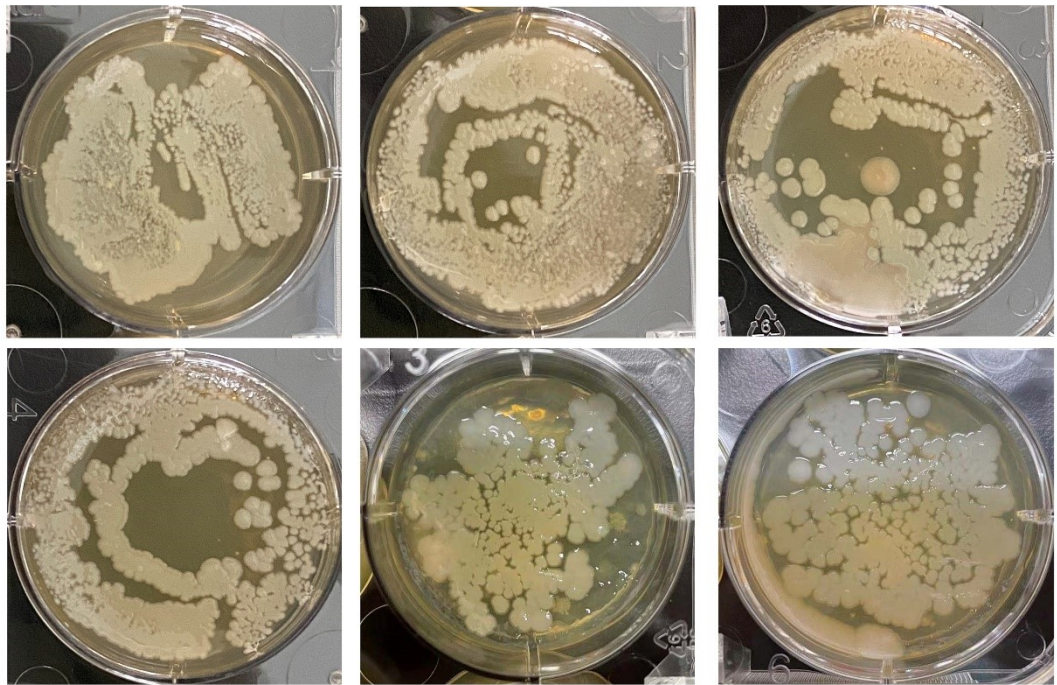


Figure S19. Standard plate counting of *S. aureus* in wound secretions.

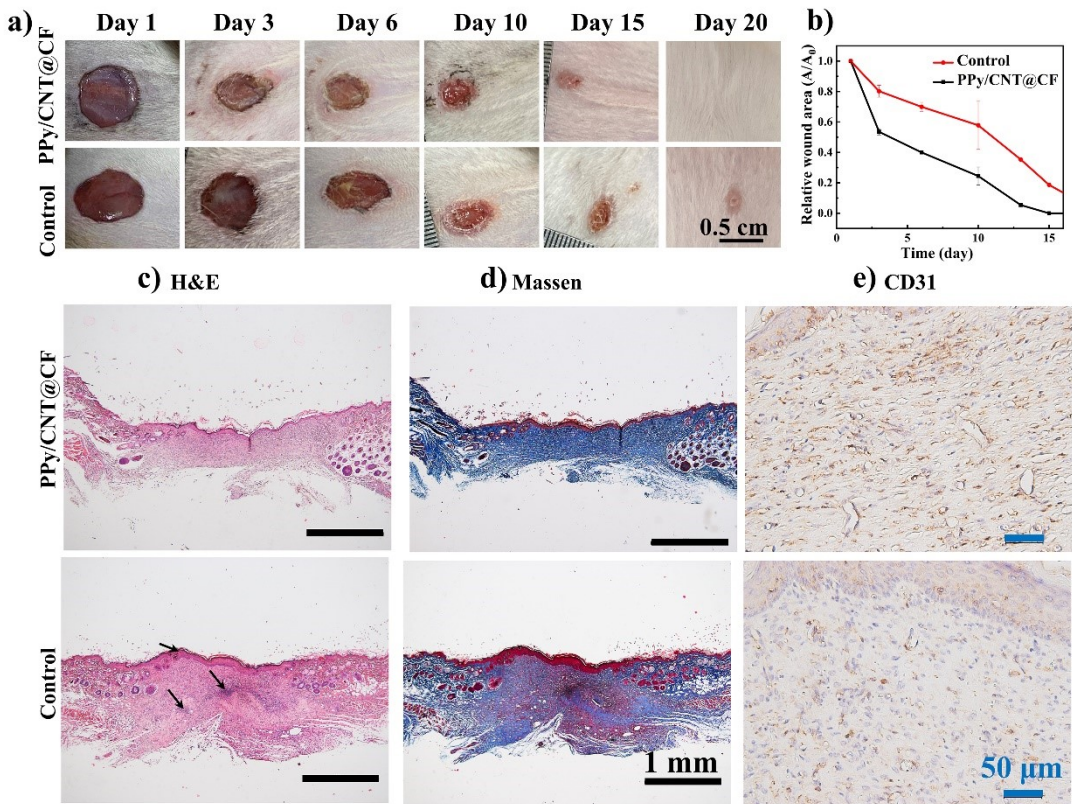


Figure S20. In vivo wound healing of PPy/CNT@CF. a) Representative photographs of the defect wounds at different days. b) Relative wound area corresponding to a. c) H&E staining, d) Masson's staining and e) immunohistochemical staining for CD31 expression of the tissue around defect wound regions collected on day 20.